

# Using a nonlocal dispersive-optical-model to generate ingredients for $\nu$ -A cross sections

Mack C. Atkinson

Washington University in St. Louis

ECT\* 2019

# Using a nonlocal dispersive-optical-model to generate ingredients for $\nu$ -A cross sections

Willem Dickhoff  
Bob Charity  
Henk Blok  
Louk Lapikás  
Hossein Mahzoon  
Cole Pruitt  
Lee Sobotka

Mack C. Atkinson

Washington University in St. Louis

ECT\* 2019

- Goal is to help describe the nuclear aspects of  $\nu$ -A interactions

- Goal is to help describe the nuclear aspects of  $\nu$ -A interactions
- The structure of large nuclei can be determined using a nonlocal dispersive optical model (DOM)

- Goal is to help describe the nuclear aspects of  $\nu$ -A interactions
- The structure of large nuclei can be determined using a nonlocal dispersive optical model (DOM)
- Experimental data is used to constrain the DOM

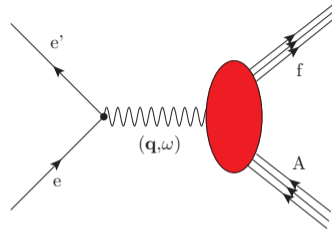
- Goal is to help describe the nuclear aspects of  $\nu$ -A interactions
- The structure of large nuclei can be determined using a nonlocal dispersive optical model (DOM)
- Experimental data is used to constrain the DOM
- The  $(e, e'p)$  reaction can be described using the DOM

- Goal is to help describe the nuclear aspects of  $\nu$ -A interactions
- The structure of large nuclei can be determined using a nonlocal dispersive optical model (DOM)
- Experimental data is used to constrain the DOM
- The  $(e, e'p)$  reaction can be described using the DOM
- This can be extended to different leptonic probes

- Goal is to help describe the nuclear aspects of  $\nu$ -A interactions
- The structure of large nuclei can be determined using a nonlocal dispersive optical model (DOM)
- Experimental data is used to constrain the DOM
- The  $(e, e'p)$  reaction can be described using the DOM
- This can be extended to different leptonic probes
- In particular, a DOM analysis of  $^{40}\text{Ar}$  (relevant for DUNE) is underway

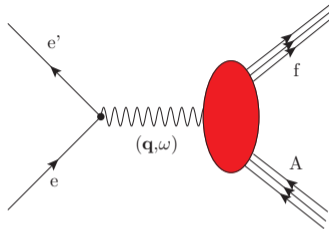


# Electron-Nucleus Scattering



# Electron-Nucleus Scattering

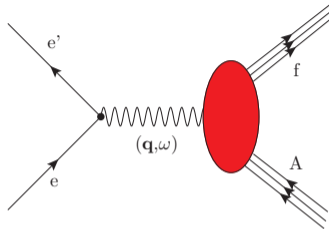
$$\frac{d^2\sigma}{d\Omega dE} = L_{\mu\nu} W^{\mu\nu}$$



# Electron-Nucleus Scattering

$$\frac{d^2\sigma}{d\Omega dE} = L_{\mu\nu} W^{\mu\nu}$$

- Impulse Approximation (IA)  $\implies$  one-body current

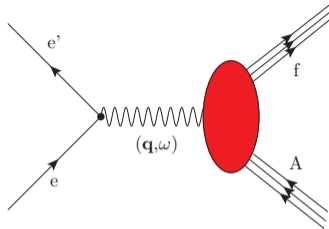


# Electron-Nucleus Scattering

$$\frac{d^2\sigma}{d\Omega dE} = L_{\mu\nu} W^{\mu\nu}$$

- Impulse Approximation (IA)  $\implies$  one-body current

$$W^{\mu\nu} \propto \text{Im}\Pi(\mathbf{q}, \omega) \quad (\text{Polarization Propagator})$$



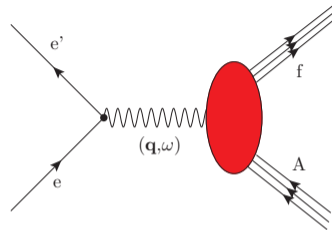
# Electron-Nucleus Scattering

$$\frac{d^2\sigma}{d\Omega dE} = L_{\mu\nu} W^{\mu\nu}$$

- Impulse Approximation (IA)  $\implies$  one-body current

$$W^{\mu\nu} \propto \text{Im}\Pi(\mathbf{q}, \omega) \quad (\text{Polarization Propagator})$$

Fermi-Gas



# Electron-Nucleus Scattering

$$\frac{d^2\sigma}{d\Omega dE} = L_{\mu\nu} W^{\mu\nu}$$

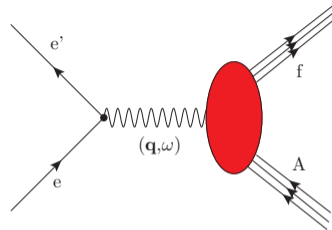
- Impulse Approximation (IA)  $\implies$  one-body current

$$W^{\mu\nu} \propto \text{Im}\Pi(\mathbf{q}, \omega) \quad (\text{Polarization Propagator})$$

Fermi-Gas



PWIA



# Electron-Nucleus Scattering

$$\frac{d^2\sigma}{d\Omega dE} = L_{\mu\nu} W^{\mu\nu}$$

- Impulse Approximation (IA)  $\implies$  one-body current

$$W^{\mu\nu} \propto \text{Im}\Pi(\mathbf{q}, \omega) \quad (\text{Polarization Propagator})$$

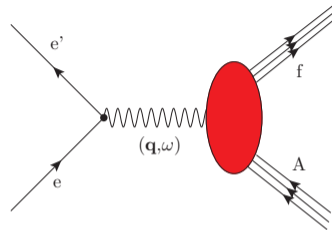
Fermi-Gas



PWIA



DWIA



# Single-Particle Propagator and the Dyson Equation

$$G_{lj}(r, r'; E) = \sum_m \frac{\langle \Psi_0^A | a_{rlj} | \Psi_m^{A+1} \rangle \langle \Psi_m^{A+1} | a_{r'lj}^\dagger | \Psi_0^A \rangle}{E - (E_m^{A+1} - E_0^A) + i\eta} + \sum_n \frac{\langle \Psi_0^A | a_{r'lj}^\dagger | \Psi_n^{A-1} \rangle \langle \Psi_n^{A-1} | a_{rlj} | \Psi_0^A \rangle}{E - (E_0^A - E_n^{A-1}) - i\eta}$$



# Single-Particle Propagator and the Dyson Equation

$$G_{lj}(r, r'; E) = \sum_m \frac{\langle \Psi_0^A | a_{rlj} | \Psi_m^{A+1} \rangle \langle \Psi_m^{A+1} | a_{r'lj}^\dagger | \Psi_0^A \rangle}{E - (E_m^{A+1} - E_0^A) + i\eta} + \sum_n \frac{\langle \Psi_0^A | a_{r'lj}^\dagger | \Psi_n^{A-1} \rangle \langle \Psi_n^{A-1} | a_{rlj} | \Psi_0^A \rangle}{E - (E_0^A - E_n^{A-1}) - i\eta}$$

- Poles correspond to excitation energies of  $(A + 1)$  or  $(A - 1)$  nucleus

# Single-Particle Propagator and the Dyson Equation

$$G_{lj}(r, r'; E) = \sum_m \frac{\langle \Psi_0^A | a_{rlj} | \Psi_m^{A+1} \rangle \langle \Psi_m^{A+1} | a_{r'lj}^\dagger | \Psi_0^A \rangle}{E - (E_m^{A+1} - E_0^A) + i\eta} + \sum_n \frac{\langle \Psi_0^A | a_{r'lj}^\dagger | \Psi_n^{A-1} \rangle \langle \Psi_n^{A-1} | a_{rlj} | \Psi_0^A \rangle}{E - (E_0^A - E_n^{A-1}) - i\eta}$$

- Poles correspond to excitation energies of  $(A + 1)$  or  $(A - 1)$  nucleus
- Numerator like a transition probability to given excitation

# Single-Particle Propagator and the Dyson Equation

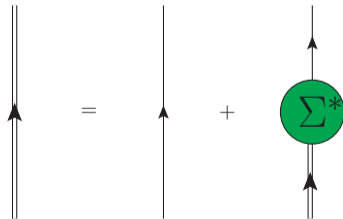
$$G_{lj}(r, r'; E) = \sum_m \frac{\langle \Psi_0^A | a_{rlj} | \Psi_m^{A+1} \rangle \langle \Psi_m^{A+1} | a_{r'lj}^\dagger | \Psi_0^A \rangle}{E - (E_m^{A+1} - E_0^A) + i\eta} + \sum_n \frac{\langle \Psi_0^A | a_{r'lj}^\dagger | \Psi_n^{A-1} \rangle \langle \Psi_n^{A-1} | a_{rlj} | \Psi_0^A \rangle}{E - (E_0^A - E_n^{A-1}) - i\eta}$$

- Poles correspond to excitation energies of  $(A + 1)$  or  $(A - 1)$  nucleus
- Numerator like a transition probability to given excitation
- Close connection with experimental observables

# Single-Particle Propagator and the Dyson Equation

$$G_{lj}(r, r'; E) = \sum_m \frac{\langle \Psi_0^A | a_{rlj} | \Psi_m^{A+1} \rangle \langle \Psi_m^{A+1} | a_{r'lj}^\dagger | \Psi_0^A \rangle}{E - (E_m^{A+1} - E_0^A) + i\eta} + \sum_n \frac{\langle \Psi_0^A | a_{r'lj}^\dagger | \Psi_n^{A-1} \rangle \langle \Psi_n^{A-1} | a_{rlj} | \Psi_0^A \rangle}{E - (E_0^A - E_n^{A-1}) - i\eta}$$

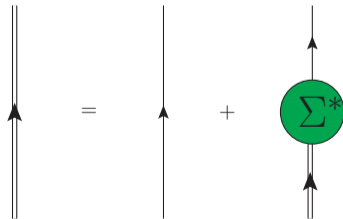
- Poles correspond to excitation energies of  $(A + 1)$  or  $(A - 1)$  nucleus
- Numerator like a transition probability to given excitation
- Close connection with experimental observables
- Perturbation expansion of  $G$  leads to the Dyson equation



# Single-Particle Propagator and the Dyson Equation

$$G_{lj}(r, r'; E) = \sum_m \frac{\langle \Psi_0^A | a_{rlj} | \Psi_m^{A+1} \rangle \langle \Psi_m^{A+1} | a_{r'lj}^\dagger | \Psi_0^A \rangle}{E - (E_m^{A+1} - E_0^A) + i\eta} + \sum_n \frac{\langle \Psi_0^A | a_{r'lj}^\dagger | \Psi_n^{A-1} \rangle \langle \Psi_n^{A-1} | a_{rlj} | \Psi_0^A \rangle}{E - (E_0^A - E_n^{A-1}) - i\eta}$$

- Poles correspond to excitation energies of  $(A + 1)$  or  $(A - 1)$  nucleus
- Numerator like a transition probability to given excitation
- Close connection with experimental observables
- Perturbation expansion of  $G$  leads to the Dyson equation
- If the irreducible self-energy ( $\Sigma^*$ ) is known, then so is  $G$



# Spectral function

$$S_{\ell j}^h(r; E) = \frac{1}{\pi} \operatorname{Im} G_{\ell j}(r, r; E) \theta(E - (E_0^A - E_0^{A-1}))$$

# Spectral function

$$S_{\ell j}^h(r; E) = \frac{1}{\pi} \text{Im} G_{\ell j}(r, r; E) \theta(E - (E_0^A - E_0^{A-1}))$$

- Reveals effects of many-body correlations beyond the independent particle model

# Spectral function

$$S_{\ell j}^h(r; E) = \frac{1}{\pi} \text{Im} G_{\ell j}(r, r; E) \theta(E - (E_0^A - E_0^{A-1}))$$

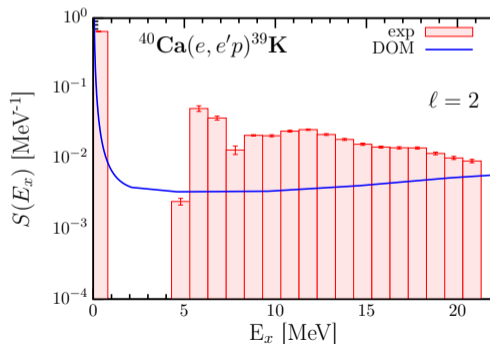
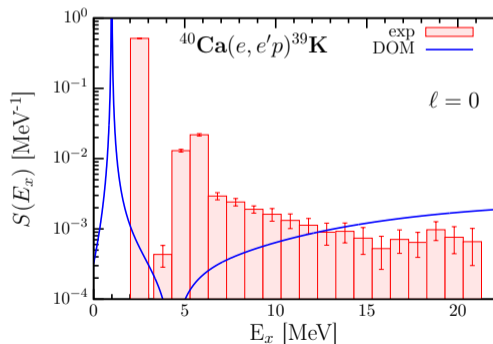
- Reveals effects of many-body correlations beyond the independent particle model
- Can be observed with excitation spectrum from knockout reactions



# Spectral function

$$S_{\ell j}^h(r; E) = \frac{1}{\pi} \text{Im} G_{\ell j}(r, r; E) \theta(E - (E_0^A - E_0^{A-1}))$$

- Reveals effects of many-body correlations beyond the independent particle model
- Can be observed with excitation spectrum from knockout reactions



# The Dispersive Optical Model (DOM)

- Irreducible self-energy at positive energies corresponds to an optical potential

# The Dispersive Optical Model (DOM)

- Irreducible self-energy at positive energies corresponds to an optical potential
- Use same functional form as standard optical potentials to parametrize self-energy

# The Dispersive Optical Model (DOM)

- Irreducible self-energy at positive energies corresponds to an optical potential
- Use same functional form as standard optical potentials to parametrize self-energy
- $\Sigma^*(\mathbf{r}, \mathbf{r}'; E)$  is explicitly **nonlocal**

# The Dispersive Optical Model (DOM)

- Irreducible self-energy at positive energies corresponds to an optical potential
- Use same functional form as standard optical potentials to parametrize self-energy
- $\Sigma^*(\mathbf{r}, \mathbf{r}'; E)$  is explicitly **nonlocal**
- Dispersion relation connects to negative energies

# The Dispersive Optical Model (DOM)

- Irreducible self-energy at positive energies corresponds to an optical potential
- Use same functional form as standard optical potentials to parametrize self-energy
- $\Sigma^*(\mathbf{r}, \mathbf{r}'; E)$  is explicitly **nonlocal**
- Dispersion relation connects to negative energies

## Dispersive Correction

$$\begin{aligned} \text{Re}\Sigma_{\ell j}(r, r'; E) = & \text{Re}\Sigma_{\ell j}(r, r'; \epsilon_F) - \frac{1}{\pi}(\epsilon_F - E)\mathcal{P} \int_{\epsilon_T^+}^{\infty} dE' \text{Im}\Sigma_{\ell j}(r, r'; E') \left[ \frac{1}{E - E'} - \frac{1}{\epsilon_F - E'} \right] \\ & + \frac{1}{\pi}(\epsilon_F - E)\mathcal{P} \int_{-\infty}^{\epsilon_T^-} dE' \text{Im}\Sigma_{\ell j}(r, r'; E') \left[ \frac{1}{E - E'} - \frac{1}{\epsilon_F - E'} \right] \end{aligned}$$

# The Dispersive Optical Model (DOM)

- Irreducible self-energy at positive energies corresponds to an optical potential
- Use same functional form as standard optical potentials to parametrize self-energy
- $\Sigma^*(\mathbf{r}, \mathbf{r}'; E)$  is explicitly **nonlocal**
- Dispersion relation connects to negative energies

## Dispersive Correction

$$\begin{aligned} \text{Re}\Sigma_{\ell j}(r, r'; E) = & \text{Re}\Sigma_{\ell j}(r, r'; \epsilon_F) - \frac{1}{\pi}(\epsilon_F - E)\mathcal{P} \int_{\epsilon_T^+}^{\infty} dE' \text{Im}\Sigma_{\ell j}(r, r'; E') \left[ \frac{1}{E - E'} - \frac{1}{\epsilon_F - E'} \right] \\ & + \frac{1}{\pi}(\epsilon_F - E)\mathcal{P} \int_{-\infty}^{\epsilon_T^-} dE' \text{Im}\Sigma_{\ell j}(r, r'; E') \left[ \frac{1}{E - E'} - \frac{1}{\epsilon_F - E'} \right] \end{aligned}$$

- This constraint ensures bound and scattering quantities are simultaneously described

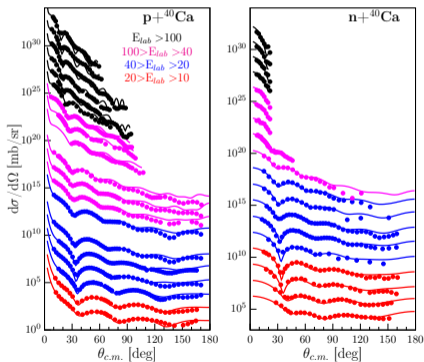
# Fitting the Self-energy ( $^{40}\text{Ca}$ )

- Parameters of self-energy varied to minimize  $\chi^2$



# Fitting the Self-energy ( $^{40}\text{Ca}$ )

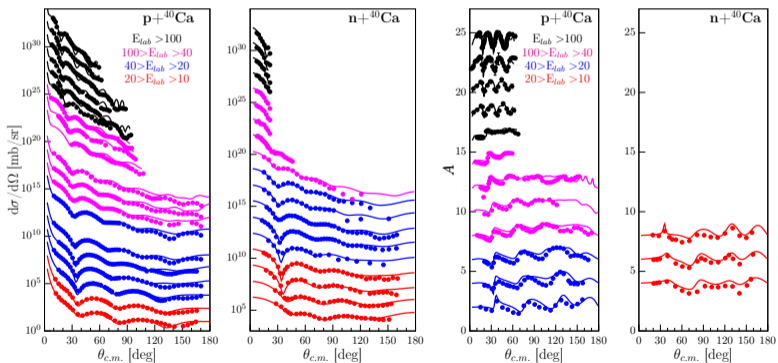
- Parameters of self-energy varied to minimize  $\chi^2$



Data: J.M. Mueller et al. *Phys. Rev. C*, **83** 064605, 2011

# Fitting the Self-energy ( $^{40}\text{Ca}$ )

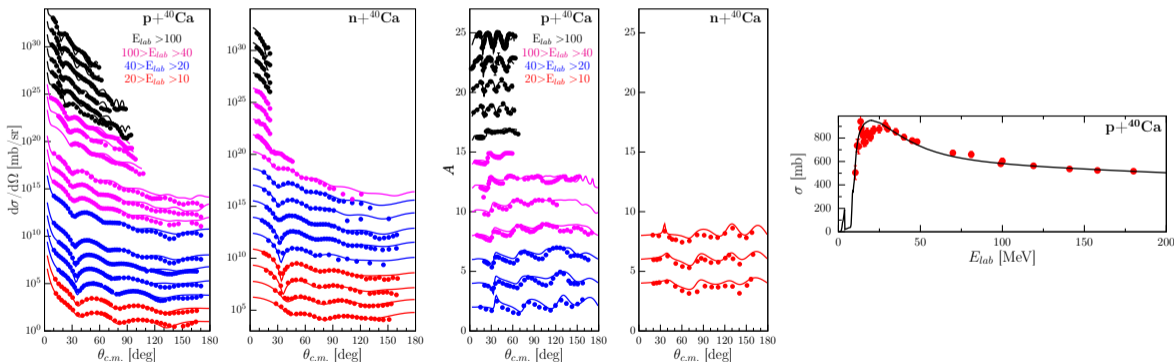
- Parameters of self-energy varied to minimize  $\chi^2$



Data: J.M. Mueller et al. *Phys. Rev. C*, **83** 064605, 2011

# Fitting the Self-energy ( $^{40}\text{Ca}$ )

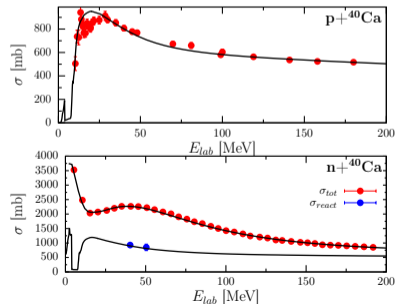
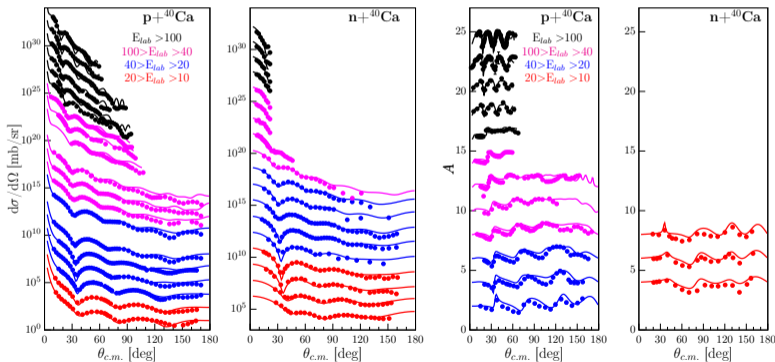
- Parameters of self-energy varied to minimize  $\chi^2$



Data: J.M. Mueller et al. *Phys. Rev. C*, **83** 064605, 2011

# Fitting the Self-energy ( $^{40}\text{Ca}$ )

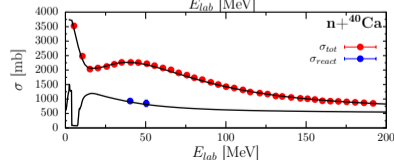
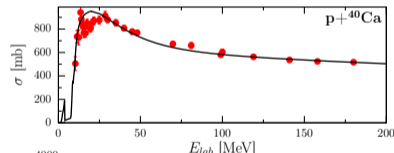
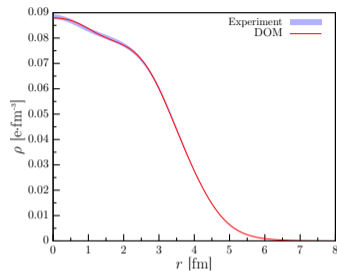
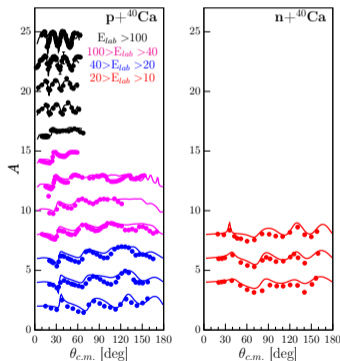
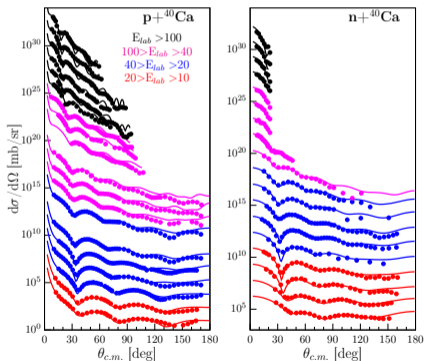
- Parameters of self-energy varied to minimize  $\chi^2$



Data: J.M. Mueller et al. *Phys. Rev. C*, **83** 064605, 2011

# Fitting the Self-energy ( $^{40}\text{Ca}$ )

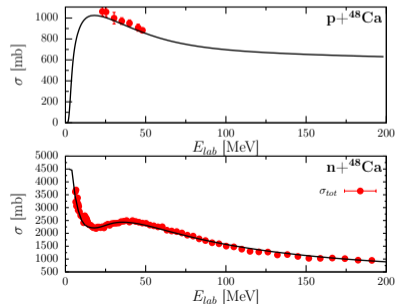
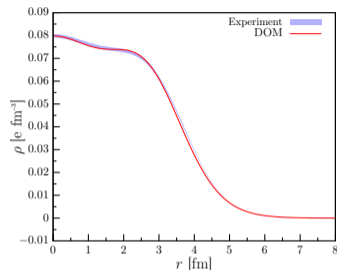
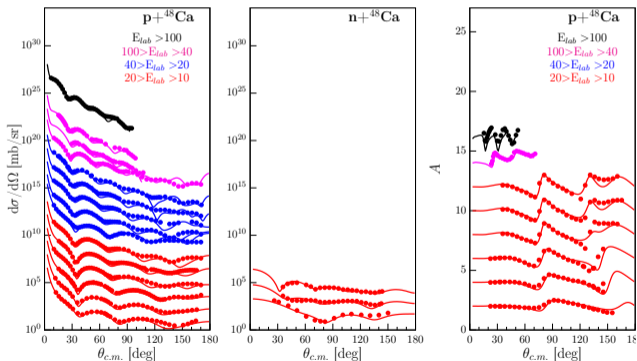
- Parameters of self-energy varied to minimize  $\chi^2$
- Reproducing the data means self-energy is found



Data: J.M. Mueller et al. *Phys. Rev. C*, **83** 064605, 2011

# Fitting the Self-energy ( $^{48}\text{Ca}$ )

- Parameters of self-energy varied to minimize  $\chi^2$
- Reproducing the data means self-energy is found

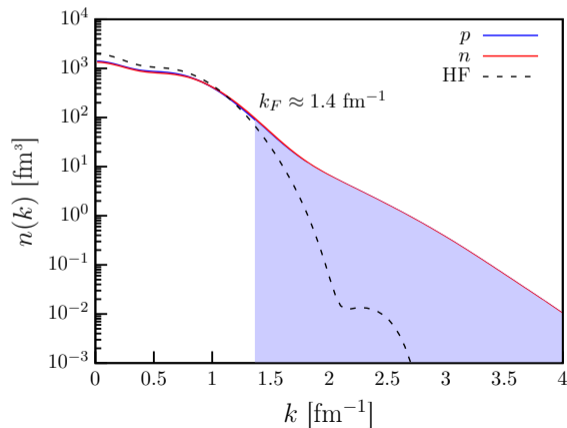


Data: J.M. Mueller et al. *Phys. Rev. C*, **83** 064605, 2011

# Momentum Distributions

$$n(\mathbf{k}) = \int d^3r \int d^3r' e^{i\mathbf{k}\cdot(\mathbf{r}-\mathbf{r}')} \rho(\mathbf{r}, \mathbf{r}')$$

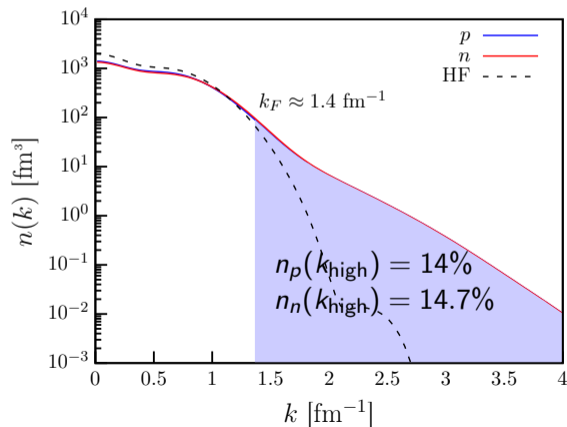
$^{40}\text{Ca}$  DOM Single-Particle Momentum Distribution



# Momentum Distributions

$$n(\mathbf{k}) = \int d^3r \int d^3r' e^{i\mathbf{k}\cdot(\mathbf{r}-\mathbf{r}')} \rho(\mathbf{r}, \mathbf{r}')$$

$^{40}\text{Ca}$  DOM Single-Particle Momentum Distribution

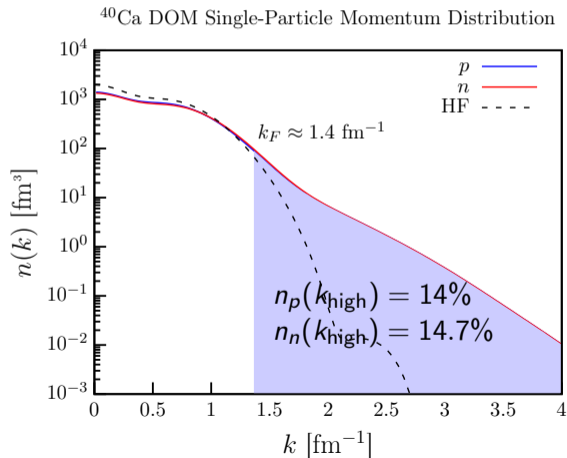




# Momentum Distributions

- Short-range correlations (SRC) responsible for this high-momentum content

$$n(\mathbf{k}) = \int d^3r \int d^3r' e^{i\mathbf{k}\cdot(\mathbf{r}-\mathbf{r}')} \rho(\mathbf{r}, \mathbf{r}')$$

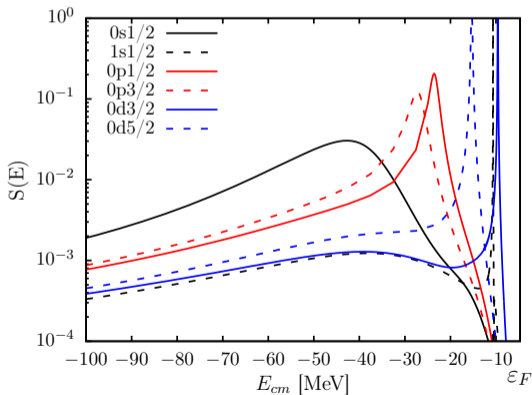


# Momentum Distributions

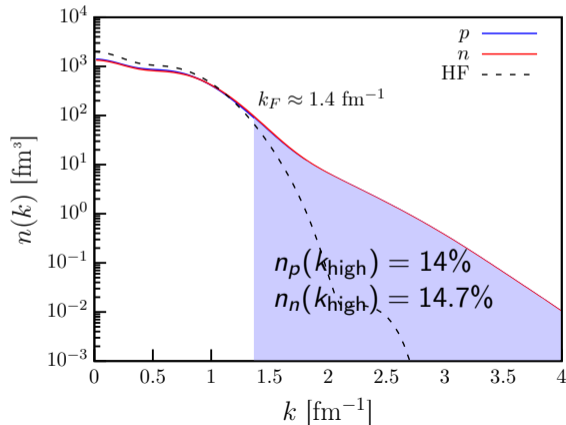
- Short-range correlations (SRC) responsible for this high-momentum content

$$n(\mathbf{k}) = \int d^3r \int d^3r' e^{i\mathbf{k}\cdot(\mathbf{r}-\mathbf{r}')} \rho(\mathbf{r}, \mathbf{r}')$$

Proton Spectral Functions in  $^{40}\text{Ca}$



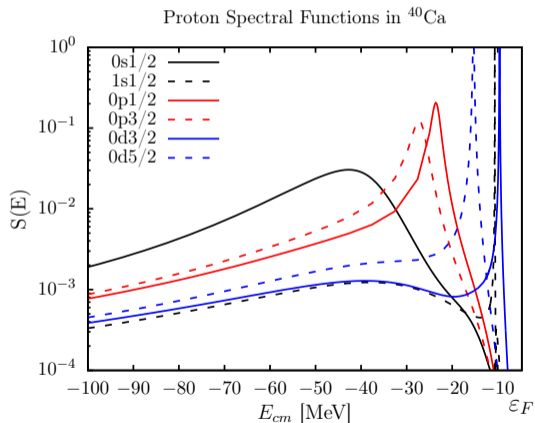
$^{40}\text{Ca}$  DOM Single-Particle Momentum Distribution



# Constraints for Spectral Function

$$S^h(\alpha, \beta; E) = \frac{1}{\pi} \text{Im}\{G(\alpha, \beta; E)\}$$

$$S^h(E) = \sum_{\alpha} S(\alpha, \alpha; E)$$



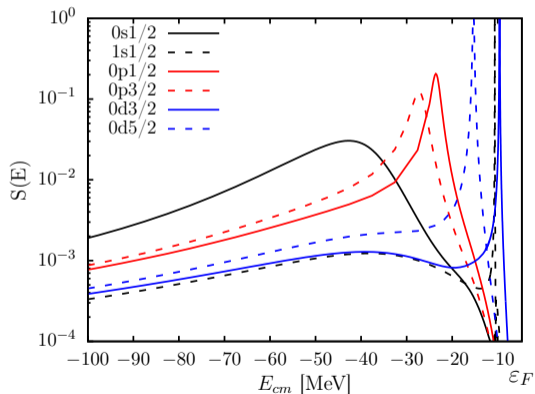
# Constraints for Spectral Function

$$S^h(\alpha, \beta; E) = \frac{1}{\pi} \text{Im}\{G(\alpha, \beta; E)\}$$

$$S^h(E) = \sum_{\alpha} S(\alpha, \alpha; E)$$

$$\rho_{\alpha, \beta} = \int_{-\infty}^{\epsilon_F} dE S(\alpha, \beta; E)$$

Proton Spectral Functions in  $^{40}\text{Ca}$



# Constraints for Spectral Function

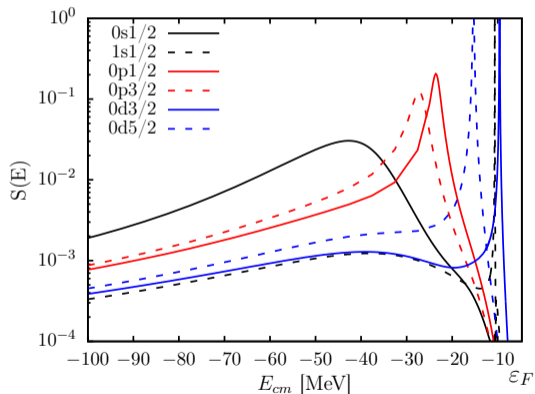
$$S^h(\alpha, \beta; E) = \frac{1}{\pi} \text{Im}\{G(\alpha, \beta; E)\}$$

$$S^h(E) = \sum_{\alpha} S(\alpha, \alpha; E)$$

$$\rho_{\alpha, \beta} = \int_{-\infty}^{\epsilon_F} dE S(\alpha, \beta; E)$$

$$N, Z = \sum_{\alpha} \rho_{\alpha, \alpha}^{N, Z}$$

Proton Spectral Functions in  $^{40}\text{Ca}$



# Constraints for Spectral Function

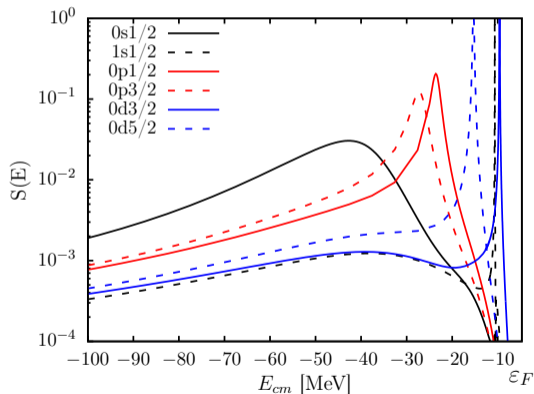
$$S^h(\alpha, \beta; E) = \frac{1}{\pi} \text{Im}\{G(\alpha, \beta; E)\}$$

$$S^h(E) = \sum_{\alpha} S(\alpha, \alpha; E)$$

$$\rho_{\alpha, \beta} = \int_{-\infty}^{\epsilon_F} dE S(\alpha, \beta; E) \quad N, Z = \sum_{\alpha} \rho_{\alpha, \alpha}^{N, Z}$$

$$E_0^A = \frac{1}{2} \sum_{\alpha \beta} \left[ T_{\beta \alpha} \rho_{\alpha \beta} + \delta_{\alpha \beta} \int_{-\infty}^{\epsilon_f^-} dE E S_h(\alpha; E) \right]$$

Proton Spectral Functions in  $^{40}\text{Ca}$



# Constraints for Spectral Function

$$S^h(\alpha, \beta; E) = \frac{1}{\pi} \text{Im}\{G(\alpha, \beta; E)\}$$

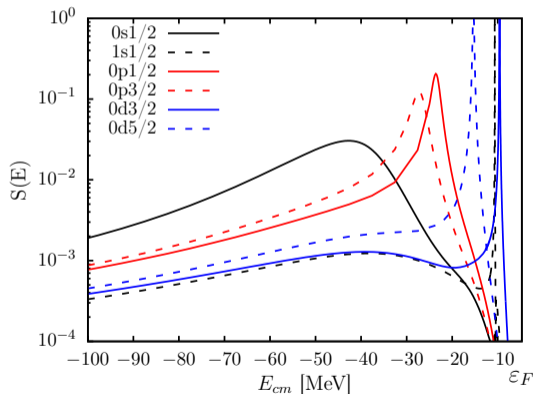
$$S^h(E) = \sum_{\alpha} S(\alpha, \alpha; E)$$

$$\rho_{\alpha, \beta} = \int_{-\infty}^{\epsilon_F} dE S(\alpha, \beta; E) \quad N, Z = \sum_{\alpha} \rho_{\alpha, \alpha}^{N, Z}$$

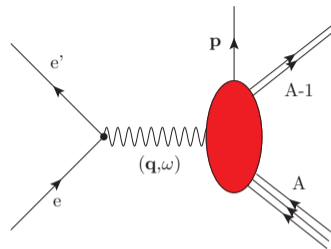
$$E_0^A = \frac{1}{2} \sum_{\alpha\beta} \left[ T_{\beta\alpha} \rho_{\alpha\beta} + \delta_{\alpha\beta} \int_{-\infty}^{\epsilon_f^-} dE E S_h(\alpha; E) \right]$$

	N	Z	DOM $E_0^A/A$	Exp. $E_0^A/A$
$^{40}\text{Ca}$	19.9	19.8	-8.49	-8.55
$^{48}\text{Ca}$	27.9	19.9	-8.7	-8.66

Proton Spectral Functions in  $^{40}\text{Ca}$



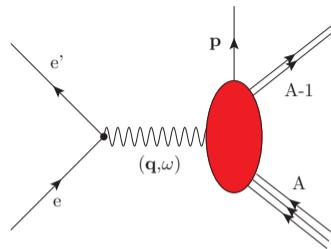
# DWIA for exclusive $^{40}\text{Ca}(e, e'p)^{39}\text{K}$ reaction





# DWIA for exclusive $^{40}\text{Ca}(e, e'p)^{39}\text{K}$ reaction

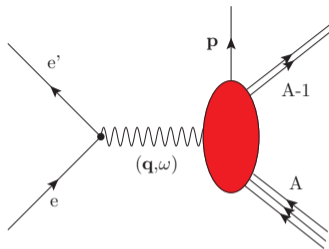
- DWIA for exclusive reaction (C. Giusti's DWEEPY code)



# DWIA for exclusive $^{40}\text{Ca}(e, e'p)^{39}\text{K}$ reaction

- DWIA for exclusive reaction (C. Giusti's DWEEPY code)

$$J^\mu(\mathbf{q}) = \int \chi_{E\alpha}^{(-)*}(\mathbf{r}) j^\mu(\mathbf{r}) \phi_{E\alpha}(\mathbf{r}) [\mathcal{Z}_\alpha(E)]^{1/2} e^{i\mathbf{q}\cdot\mathbf{r}} d^3r$$

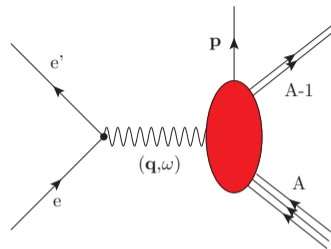


# DWIA for exclusive $^{40}\text{Ca}(e, e'p)^{39}\text{K}$ reaction

- DWIA for exclusive reaction (C. Giusti's DWEEPY code)

$$J^\mu(\mathbf{q}) = \int \chi_{E\alpha}^{(-)*}(\mathbf{r}) j^\mu(\mathbf{r}) \phi_{E\alpha}(\mathbf{r}) [\mathcal{Z}_\alpha(E)]^{1/2} e^{i\mathbf{q}\cdot\mathbf{r}} d^3r$$

- Spectroscopic factor,  $\mathcal{Z}$ , quantifies correlations

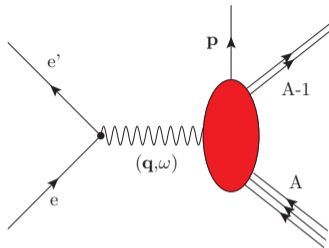


# DWIA for exclusive $^{40}\text{Ca}(e, e'p)^{39}\text{K}$ reaction

- DWIA for exclusive reaction (C. Giusti's DWEEPY code)

$$J^\mu(\mathbf{q}) = \int \chi_{E\alpha}^{(-)*}(\mathbf{r}) j^\mu(\mathbf{r}) \phi_{E\alpha}(\mathbf{r}) [\mathcal{Z}_\alpha(E)]^{1/2} e^{i\mathbf{q}\cdot\mathbf{r}} d^3r$$

- Spectroscopic factor,  $\mathcal{Z}$ , quantifies correlations
- DOM provides all ingredients

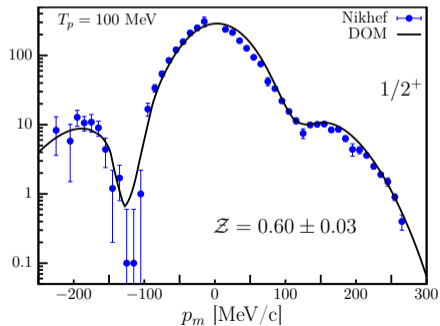
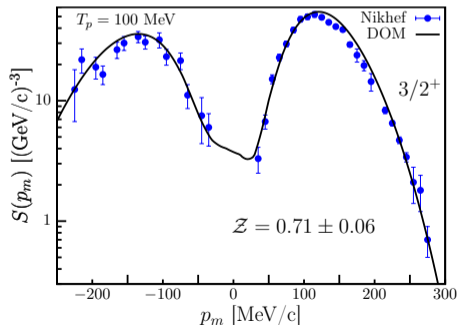
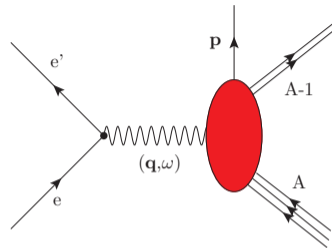


# DWIA for exclusive $^{40}\text{Ca}(e, e'p)^{39}\text{K}$ reaction

- DWIA for exclusive reaction (C. Giusti's DWEEPY code)

$$J^\mu(\mathbf{q}) = \int \chi_{E\alpha}^{(-)*}(\mathbf{r}) j^\mu(\mathbf{r}) \phi_{E\alpha}(\mathbf{r}) [\mathcal{Z}_\alpha(E)]^{1/2} e^{i\mathbf{q}\cdot\mathbf{r}} d^3r$$

- Spectroscopic factor,  $\mathcal{Z}$ , quantifies correlations
- DOM provides all ingredients

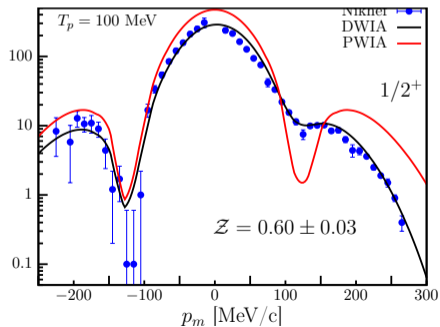
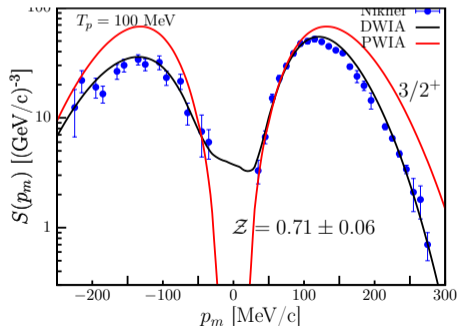
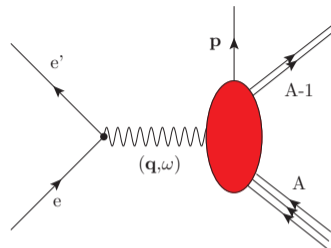


# DWIA for exclusive $^{40}\text{Ca}(e, e'p)^{39}\text{K}$ reaction

- DWIA for exclusive reaction (C. Giusti's DWEEPY code)

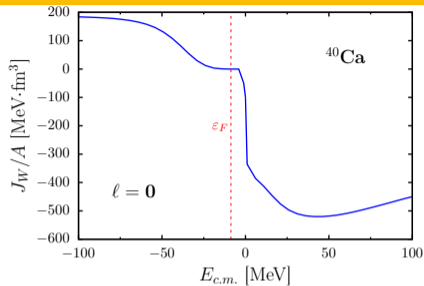
$$J^\mu(\mathbf{q}) = \int \chi_{E\alpha}^{(-)*}(\mathbf{r}) j^\mu(\mathbf{r}) \phi_{E\alpha}(\mathbf{r}) [Z_\alpha(E)]^{1/2} e^{i\mathbf{q}\cdot\mathbf{r}} d^3r$$

- Spectroscopic factor,  $Z$ , quantifies correlations
- DOM provides all ingredients



# Spectroscopic factor, Occupation, and Depletion

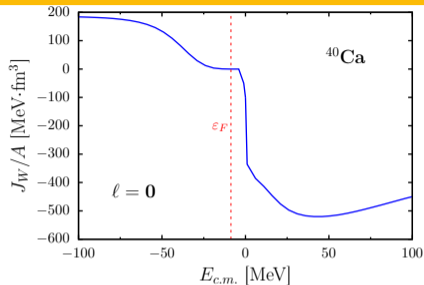
- No imaginary component of  $\Sigma^*$  around  $\epsilon_F$



# Spectroscopic factor, Occupation, and Depletion

- No imaginary component of  $\Sigma^*$  around  $\epsilon_F$
- Spectroscopic factor for states near  $\epsilon_F$  is well defined from  $\Sigma^*$

$$\mathcal{Z} = \left( 1 - \frac{\partial \Sigma^*(\alpha_{qh}, \alpha_{qh}; E)}{\partial E} \Big|_{\epsilon} \right)^{-1}$$

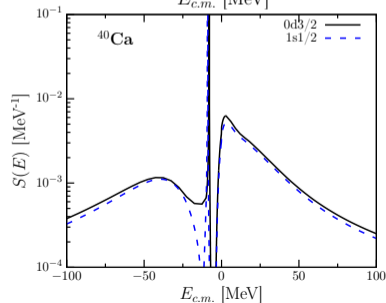
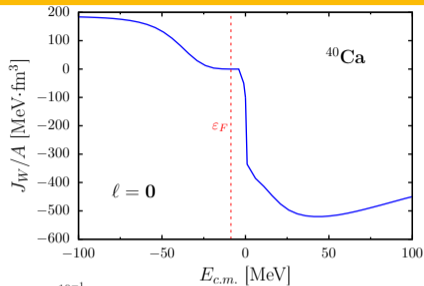




# Spectroscopic factor, Occupation, and Depletion

- No imaginary component of  $\Sigma^*$  around  $\epsilon_F$
- Spectroscopic factor for states near  $\epsilon_F$  is well defined from  $\Sigma^*$

$$\mathcal{Z} = \left( 1 - \frac{\partial \Sigma^*(\alpha_{qh}, \alpha_{qh}; E)}{\partial E} \Big|_{\epsilon} \right)^{-1}$$

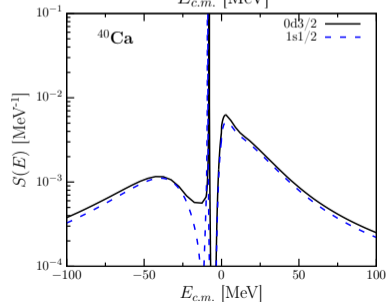
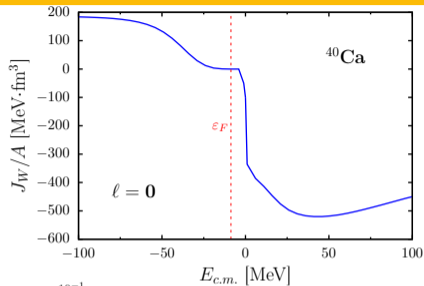


# Spectroscopic factor, Occupation, and Depletion

- No imaginary component of  $\Sigma^*$  around  $\epsilon_F$
- Spectroscopic factor for states near  $\epsilon_F$  is well defined from  $\Sigma^*$

$$\mathcal{Z} = \left( 1 - \frac{\partial \Sigma^*(\alpha_{qh}, \alpha_{qh}; E)}{\partial E} \Big|_{\epsilon} \right)^{-1}$$

$$n_{nlj} = \int_{-\infty}^{\epsilon_F} dE S_{nlj}^h(E) \quad d_{nlj} = \int_{\epsilon_F}^{\infty} dE S_{nlj}^p(E)$$



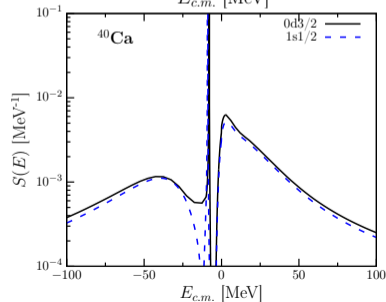
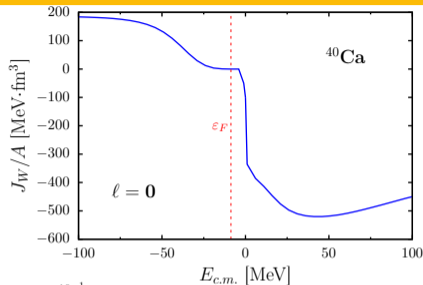
# Spectroscopic factor, Occupation, and Depletion

- No imaginary component of  $\Sigma^*$  around  $\epsilon_F$
- Spectroscopic factor for states near  $\epsilon_F$  is well defined from  $\Sigma^*$

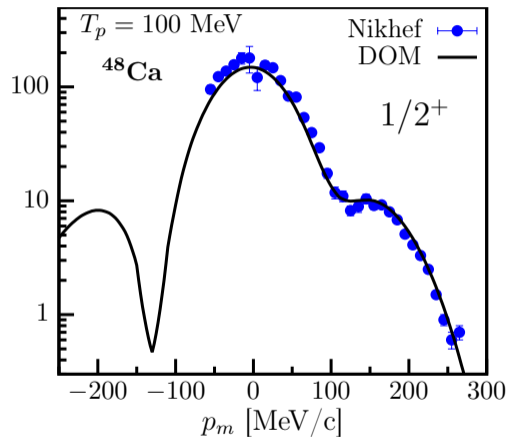
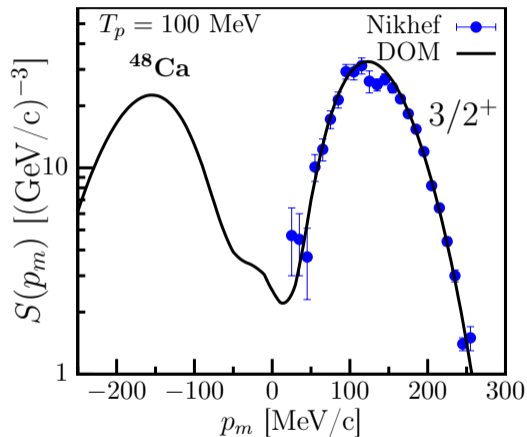
$$\mathcal{Z} = \left( 1 - \frac{\partial \Sigma^*(\alpha_{qh}, \alpha_{qh}; E)}{\partial E} \bigg|_{\epsilon} \right)^{-1}$$

$$n_{nlj} = \int_{-\infty}^{\epsilon_F} dE S_{nlj}^h(E) \quad d_{nlj} = \int_{\epsilon_F}^{\infty} dE S_{nlj}^p(E)$$

Orbital	$\mathcal{Z}$	$n_{nlj}$	$d_{nlj}$
$0d_{3/2}$	0.71	0.80	0.17
$1s_{1/2}$	0.60	0.82	0.15



# $^{48}\text{Ca}(e,e'p)^{47}\text{K}$ Momentum Distribution



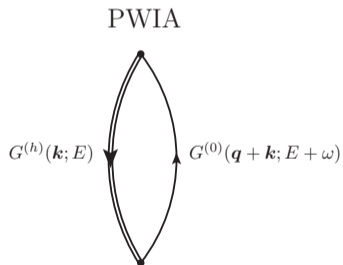
Data: G. J. Kramer et. al, Nucl. Phys. A, **679**, 267 (2001)

# Extending to inclusive cross section

- First implement PWIA
- Using DWIA for inclusive cross section will involve energies that require a relativistic treatment

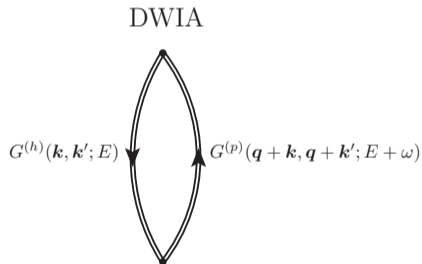
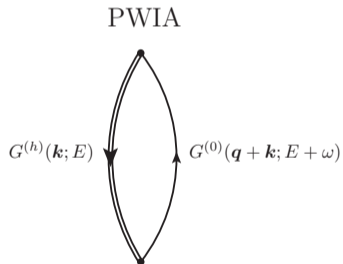
# Extending to inclusive cross section

- First implement PWIA
- Using DWIA for inclusive cross section will involve energies that require a relativistic treatment

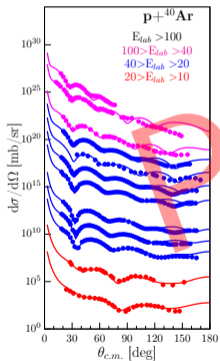


# Extending to inclusive cross section

- First implement PWIA
- Using DWIA for inclusive cross section will involve energies that require a relativistic treatment

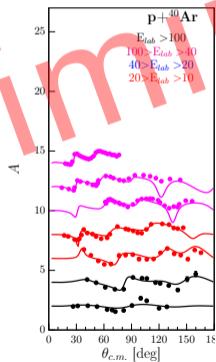
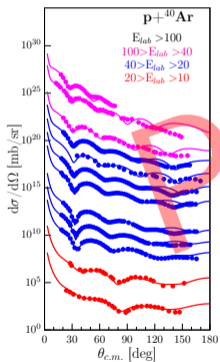


# Preliminary Fit of $^{40}\text{Ar}$

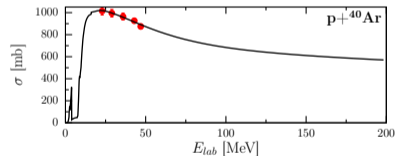
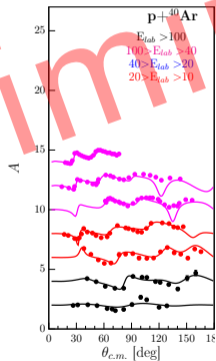
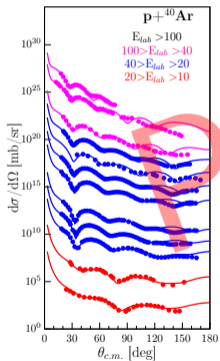




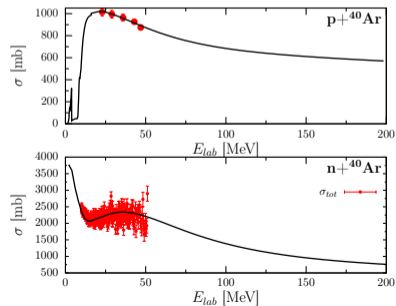
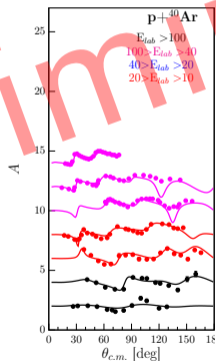
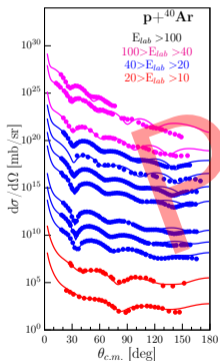
# Preliminary Fit of $^{40}\text{Ar}$



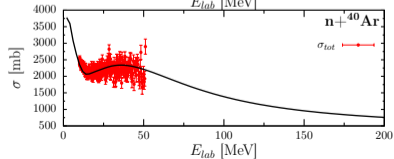
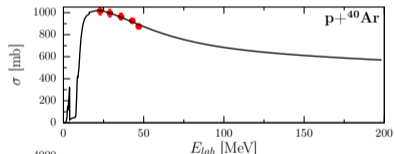
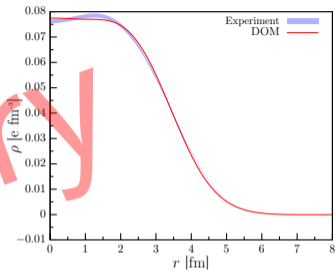
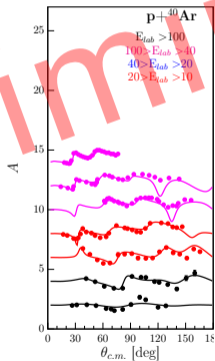
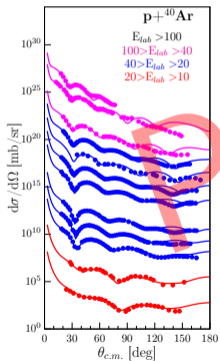
# Preliminary Fit of $^{40}\text{Ar}$



# Preliminary Fit of $^{40}\text{Ar}$



# Preliminary Fit of $^{40}\text{Ar}$



- The DOM is a robust model that can describe both positive and negative energy data

# Conclusions and Outlook

- The DOM is a robust model that can describe both positive and negative energy data
- The DOM provides a consistent description of  $^{40}\text{Ca}(e,e'p)^{39}\text{K}$  data

# Conclusions and Outlook

- The DOM is a robust model that can describe both positive and negative energy data
- The DOM provides a consistent description of  $^{40}\text{Ca}(e,e'p)^{39}\text{K}$  data
- Since this works for electrons, it should work for neutrinos

# Conclusions and Outlook

- The DOM is a robust model that can describe both positive and negative energy data
- The DOM provides a consistent description of  $^{40}\text{Ca}(e,e'p)^{39}\text{K}$  data
- Since this works for electrons, it should work for neutrinos
- DOM analysis of  $^{40}\text{Ar}$  is underway



# Thanks

- Willem Dickhoff - Advisor
- Robert Charity - DOM and data for DOM
- Henk Blok -  $(e, e'p)$  data at Nikhef
- Louk Lapikás -  $(e, e'p)$  data at Nikhef
- Carlotta Giusti - DWEOPY Code
- Hossein Mahzoon - DOM
- Lee Sobotka - Data for DOM



# Backup

- “Smearing” of self-energy poles inflates  $\mathcal{Z}$
- Renormalize with experimental excitation energy spectrum

$$\frac{\mathcal{Z}_F^{\text{DOM}}}{\int dE S^{\text{DOM}}(E)} = \frac{\mathcal{Z}_F^{\text{exp}}}{\int dE S^{\text{exp}}(E)}$$

